

Structure and magnetism of single crystal $\text{Sr}_4\text{Ru}_3\text{O}_{10}$: A ferromagnetic triple-layer ruthenate

M. K. Crawford,¹ R. L. Harlow,¹ W. Marshall,¹ Z. Li,¹ G. Cao,² R. L. Lindstrom,³ Q. Huang,^{3,4} and J. W. Lynn³

¹*DuPont Central Research and Development Department, Wilmington, Delaware 19880-0356*

²*Department of Physics and Astronomy, University of Kentucky, Lexington, Kentucky 40506*

³*NIST Center for Neutron Research, Gaithersburg, Maryland 20899*

⁴*Department of Materials and Nuclear Engineering, University of Maryland, College Park, Maryland 20742*

(Received 4 March 2002; published 22 May 2002)

We have determined the structure and magnetic properties of flux-grown single crystals of the triple-layer ruthenate $\text{Sr}_4\text{Ru}_3\text{O}_{10}$ by x-ray diffraction and magnetic susceptibility measurements, respectively. The orthorhombic unit cell has $Pbam$ space group symmetry and contains two crystallographically independent triple layers. The RuO_6 octahedra in the outer two layers of each triple layer are rotated by an average of 5.6° around the c axis, while the octahedra of the inner layers are rotated in the opposite sense by an average of 11.0° . The Curie temperature of these ferromagnetic crystals is $T_{\text{Curie}} = 105$ K, with a saturated moment of $1.0 \mu_B/\text{Ru}^{4+}$ ion. Thus $\text{Sr}_4\text{Ru}_3\text{O}_{10}$ is a layered ferromagnetic ruthenate in the Ruddlesden-Popper (R - P) series $\text{Sr}_{n+1}\text{Ru}_n\text{O}_{3n+1}$, which also includes the unconventional superconductor Sr_2RuO_4 ($n=1$), the enhanced paramagnetic metal $\text{Sr}_3\text{Ru}_2\text{O}_7$ ($n=2$), and the pseudocubic ferromagnetic metal SrRuO_3 ($n=\infty$).

DOI: 10.1103/PhysRevB.65.214412

PACS number(s): 74.70.Pq, 61.10.Nz, 61.66.Fn

The study of the structures and properties of strontium ruthenates has long been of interest to solid-state chemists and physicists.¹ Nearly 40 years ago it was discovered¹ that the distorted perovskite SrRuO_3 is a ferromagnetic metal with $T_{\text{Curie}} = 160$ K, whereas the layered ruthenate Sr_2RuO_4 was found to be metallic but not ferromagnetic. Widespread interest in the ruthenates revived after the discovery of high-temperature superconductivity.² This interest, which initially derived from the potential use of metallic ruthenates, in combination with cuprate superconductors, to fabricate S - N - S devices,³ received a boost with the discovery^{4,5} of superconductivity near 1 K in the first member of the R - P series Sr_2RuO_4 . The second member of the R - P series, $\text{Sr}_3\text{Ru}_2\text{O}_7$, was first suggested to be an antiferromagnetic metal,⁶ but subsequent neutron powder-diffraction measurements⁷ failed to find any evidence for magnetic order at temperatures above 1.6 K. More recently, $\text{Sr}_3\text{Ru}_2\text{O}_7$ has been reported to be an enhanced paramagnetic metal⁸ (for crystals grown by a floating-zone process) or a ferromagnetic metal⁹ with $T_{\text{Curie}} = 105$ K (for crystals grown using a flux technique). Finally, the third R - P series member, $\text{Sr}_4\text{Ru}_3\text{O}_{10}$, is claimed¹⁰ to be a ferromagnetic metal with $T_{\text{Curie}} = 148$ K. In this paper we report a complete determination of the crystal structure of $\text{Sr}_4\text{Ru}_3\text{O}_{10}$ and describe the magnetic properties of structurally well-characterized single crystals. These results resolve the controversy concerning the magnetic properties of $\text{Sr}_3\text{Ru}_2\text{O}_7$ and provide an example of the important relationship between structural distortions and magnetic properties in ruthenates.

Single crystals of $\text{Sr}_4\text{Ru}_3\text{O}_{10}$ were grown by heating SrCO_3 and RuO_2 , with a SrCl_2 flux, in a Pt crucible to 1500°C , and then cooling the melt at 2°C to 1350°C followed by rapid cooling to room temperature. Small (less than $100 \mu\text{g}$ up to 1 mg) single crystals of $\text{Sr}_4\text{Ru}_3\text{O}_{10}$ (as well as $\text{Sr}_3\text{Ru}_2\text{O}_7$) were separated from the mixture and subsequently identified by x-ray diffraction. The full crystal structure of one of these crystals was determined by single-crystal x-ray diffraction at a high intensity insertion device beam

line at the Advanced Photon Source at Argonne National Laboratory. Experimental details for the x-ray measurements are given in a footnote to Table I. The primary Bragg reflections could be indexed assuming a tetragonal unit cell (space-group symmetry $I4/mmm$) with dimensions of $a = b = 3.9001(3)$ and $c = 28.573(3)$ Å. In this model the in-plane oxygen atoms were displaced from their ideal lattice positions by rotations of the RuO_6 octahedra around the c axis, but it was assumed that these rotations were not correlated from one triple layer to the next. The use of the synchrotron x-ray source, however, yielded measurable intensities for a number of weak superlattice reflections that could only be indexed by enlarging the crystallographic unit cell (new in-plane cell parameters $a = b = \sqrt{2}a^*$, where a^* is the $I4/mmm$ cell parameter), and reducing the space-group symmetry from tetragonal $I4/mmm$ to orthorhombic $Pbam$. Detailed structural information and lattice parameters derived from this model are given in Table I. In this model the rotations of the RuO_6 octahedra are fully ordered between triple layers. The single crystal described in Table I also exhibited a small amount of twinning that had to be incorporated within the structural model to obtain a satisfactory fit to the measured Bragg superlattice intensities.

The $Pbam$ crystal structure of $\text{Sr}_4\text{Ru}_3\text{O}_{10}$ is shown in Fig. 1. The orthorhombic unit cell is composed of triple layers of corner-shared RuO_6 octahedra separated by double rock-salt layers of Sr-O. The most important structural feature is that the RuO_6 octahedra in the outer layers of the two crystallographically independent triple layers per unit cell are rotated in the same sense about the c axis by an average of 5.25° , while the central layers are rotated in the opposite sense by $\approx 10.6^\circ$ in each of the triple layers.

A single crystal of $\text{Sr}_4\text{Ru}_3\text{O}_{10}$ was also examined by neutron activation analysis (NAA) at the NIST Center for Neutron Research. The average Sr/Ru ratio determined by NAA was 1.39 ± 0.04 (\pm one standard deviation), within two standard deviations of the expected ratio for $\text{Sr}_4\text{Ru}_3\text{O}_{10}$ of 1.33. The larger value might be due to the incorporation of $\text{Sr}_3\text{Ru}_2\text{O}_7$ or Sr_2RuO_4 during crystal growth,¹¹ both of which have Sr/Ru ratios greater than 1.33, but transmission electron

TABLE I. Structural parameters and refinement information for $\text{Sr}_4\text{Ru}_3\text{O}_{10}$ determined from single-crystal x-ray diffraction data.^a The space group is $Pbam$ ^b with $a=b=3.9001(3)$ Å, $c=28.573$ Å.

Atom	x	y	z	U_{equ}
Ru(1)	0	0	0	0.004(1)
Ru(3)	0	0	0.1402(1)	0.004(1)
Ru(6)	0.5	0	0.3598(1)	0.004(1)
Ru(8)	0.5	0	0.5	0.004(1)
O(1)	0.2028(5)	0.2971(6)	0	0.018(1)
O(3)	0.2721(4)	0.2271(5)	0.1392(1)	0.017(1)
O(6)	0.2266(4)	0.2275(5)	0.3608(1)	0.015(1)
O(8)	0.2966(4)	0.2964(6)	0.5	0.014(1)
Sr(2)	0.5	0	0.0699(1)	0.008(1)
O(2)	0	0	0.0695(1)	0.011(2)
Sr(4)	0.5	0	0.2038(1)	0.008(1)
O(4)	0	0	0.2130(2)	0.006(1)
Sr(5)	0	0	0.2961(1)	0.008(1)
O(5)	0.5	0	0.2871(2)	0.008(1)
Sr(7)	0	0	0.4301(1)	0.008(1)
O(7)	0.5	0	0.4303(1)	0.011(2)

^aUsing a synchrotron x-ray wavelength of 0.7500 Å at an insertion device beamline with a Mar-CCD area detector, x-ray intensities for 109 423 reflections were collected at room temperature using a black square plate crystal with dimensions of $\sim 0.10 \times 0.08 \times 0.01$ mm. Indexed to a cell with $a=5.5280(11)$ Å, $b=5.5260(11)$ Å, and $c=28.651(6)$ Å using DENZO, the data was scaled and merged ($R_m=0.047$). Eliminating 60 reflections in the shadow of the beam stop, 840 unique reflections were used in the refinement of the structure (SHELXTL), converging at $R1=0.039$ and $wR2=0.133$, but only after accounting for a small amount of twinning (twin matrix: 0,1,0,1,0,0,0,-1; batch scale factor=0.86).

^bWe considered the possibility that the space group was not primitive, but instead B -centered, which would make the two triple layers per unit cell crystallographically equivalent. The primitive model was initially developed based on the fact that the $hkl(h+1=2n+1)$ reflections, which should be absent if the structure were B -centered, exhibited significant intensities. It should be noted, however, that the distribution of x-ray scattering intensities is, in fact, pseudo- B -centered, and that the structure, except for the rotations of the in-plane oxygen atoms, is also pseudo- B -centered. Structural refinements in both B -centered and primitive unit cells were performed in order to decide which was more appropriate. Attempts to refine the structure in space-group $Bbcm$, however, yielded high R -values and nonpositive definite thermal displacement parameters for several oxygen atoms as well as one of the Ru atoms. While we believe that the primitive model is correct, we also realize that crystallographic twinning could give rise to the intensities that violate the B -centering. Analysis of high-quality neutron-diffraction data for larger single crystals, or single-phase powders, is one way to resolve the subtle differences between these two structural choices.

microscopy (TEM) images with spatial resolution better than 0.19 nm have not shown evidence for intergrowths in these crystals (see Fig. 1), nor have x-ray scattering data from crushed crystals detected any phases with c axes shorter than that of $\text{Sr}_4\text{Ru}_3\text{O}_{10}$.

Magnetic susceptibility data were collected with a commercial superconducting quantum interference device (SQUID) magnetometer for single crystals whose structures were first verified by single-crystal x-ray diffraction. In Fig. 2 we show the high-field dc magnetic susceptibility of $\text{Sr}_4\text{Ru}_3\text{O}_{10}$. Curie-Weiss fits to the high-temperature inverse susceptibility, measured in a 1.0 T magnetic field, yielded a magnetic moment of $2.6 \mu_B/\text{Ru}^{4+}$ ion, and a Weiss constant $\theta_W = +130$ K, consistent with spin-1 $4d^4 \text{Ru}^{4+}$ ions which are coupled ferromagnetically. We observe little crystallographic anisotropy in these values. There is a paramagnetic to ferromagnetic¹² transition at a temperature of 105 K,

which is accompanied by the appearance of magnetic hysteresis in magnetization isotherms; some low-temperature examples are shown in Fig. 3. The data in Figs. 2 and 3 show that the direction of the ferromagnetic moment (easy axis) is parallel to the c axis. The difference between the Weiss constant and the Curie temperature shows that the ferromagnetic ordering temperature in $\text{Sr}_4\text{Ru}_3\text{O}_{10}$ is slightly suppressed below the mean-field value expected for a three-dimensional ferromagnet. It should be noted that the saturation fields ($H = 0.2 \text{ T} \parallel c, 4 \text{ T} \perp c$) are quite different from those of SrRuO_3 .¹³

In Fig. 2 the low-field dc magnetic susceptibility is also shown. The magnetic transition near 105 K has sharpened considerably in the lower field, and a significant amount of irreversibility appears at temperatures below the magnetic transition temperature, consistent with the isothermal magnetization data. Furthermore, the susceptibility data suggest the

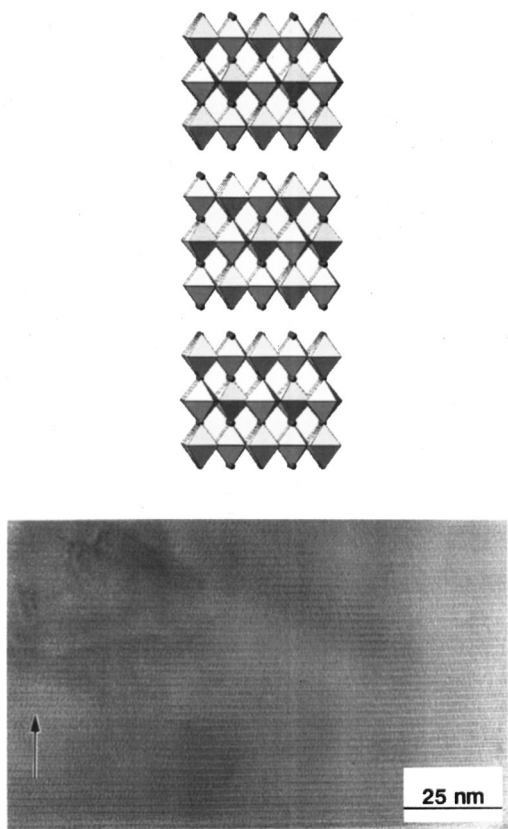


FIG. 1. (Top) Structure of the triple-layer ruthenate $\text{Sr}_4\text{Ru}_3\text{O}_{10}$. The spheres are oxygen atoms which are located on the vertices of the corner-shared RuO_6 octahedra. (bottom) TEM image of a flux-grown $\text{Sr}_4\text{Ru}_3\text{O}_{10}$ crystal. The c axis is parallel to the arrow for both pictures.

presence of a second transition below 50 K in this material. One plausible origin for this second transition is the presence of a temperature-dependent coupling between the two Ru sublattices (i.e., the central and outer Ru-O layers in each triple layer), which coaligns the spin directions in the two sublattices parallel to the c axis upon cooling below 50 K. There is also a metamagnetic like transition in the isothermal magnetization when $H \perp c$ and $T < 50$ K (an example is shown in Fig. 3 at $T = 5$ K). This transition may be related to the transition observed¹⁴ in $\text{Sr}_3\text{Ru}_2\text{O}_7$, where a paramagnetic to metamagnetic transition, producing a similar change in magnetic moment ($\sim 0.3\mu_B$), was observed at high fields and interpreted as an indication of proximity to a quantum critical point. The outer layers of $\text{Sr}_4\text{Ru}_3\text{O}_{10}$ are structurally similar to the bilayers in $\text{Sr}_3\text{Ru}_2\text{O}_7$, but the presence of the highly rotated inner layer in the triple-layer material may induce ferromagnetic order in all three layers at low temperatures.

The magnetization data in Fig. 3 show that the saturated moment is $\approx 1\mu_B$ in $\text{Sr}_4\text{Ru}_3\text{O}_{10}$ (demagnetization corrections were not made), independent of the direction of the applied magnetic field. This value is half that expected for a spin-1 ferromagnet ($g\mu_B S = 2\mu_B$), but similar to that measured in SrRuO_3 .^{1,13}

We now turn to the reported differences in magnetic properties of flux-grown and floating-zone crystals of $\text{Sr}_3\text{Ru}_2\text{O}_7$. Comparison of the magnetic properties of flux-grown $\text{Sr}_4\text{Ru}_3\text{O}_{10}$ reported in this paper, with the magnetic properties of flux-grown $\text{Sr}_3\text{Ru}_2\text{O}_7$ crystals reported previously,⁹ immediately shows that their magnetic properties are nearly identical. This observation suggests that the original samples of flux-grown $\text{Sr}_3\text{Ru}_2\text{O}_7$ contained significant amounts of

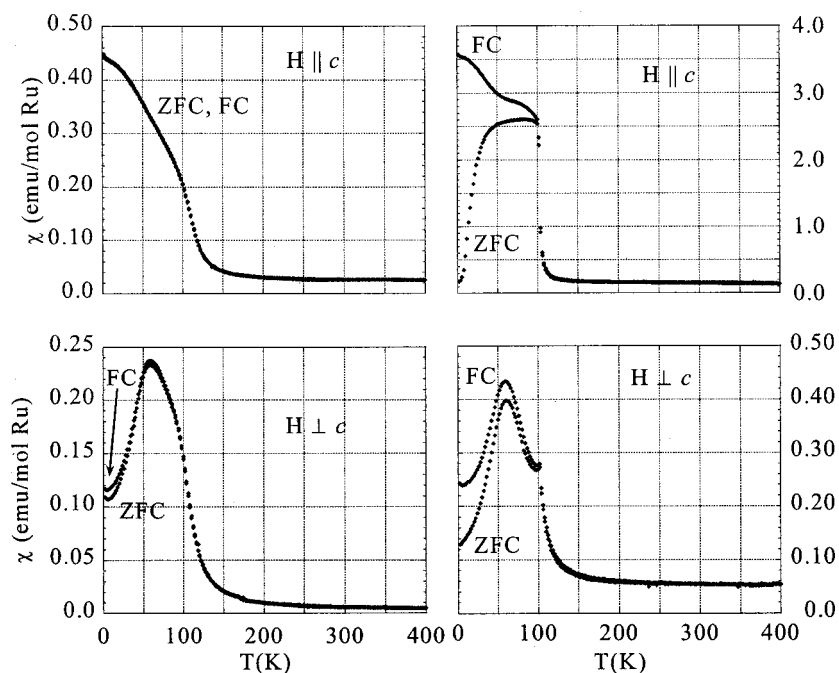


FIG. 2. (Left) High-field (1.0 T) magnetic susceptibility of a single crystal of $\text{Sr}_4\text{Ru}_3\text{O}_{10}$ measured with the magnetic field parallel to (top) or perpendicular to (bottom) the crystallographic c axis. Both zero-field-cooled (ZFC) and field-cooled (FC) data are shown for each field orientation. (Right) Low-field (0.01 T) magnetic susceptibility of a single crystal of $\text{Sr}_4\text{Ru}_3\text{O}_{10}$ measured with the magnetic field parallel to (top) or perpendicular to (bottom) the crystallographic c axis. Both zero-field and field-cooled data are shown for each field orientation.

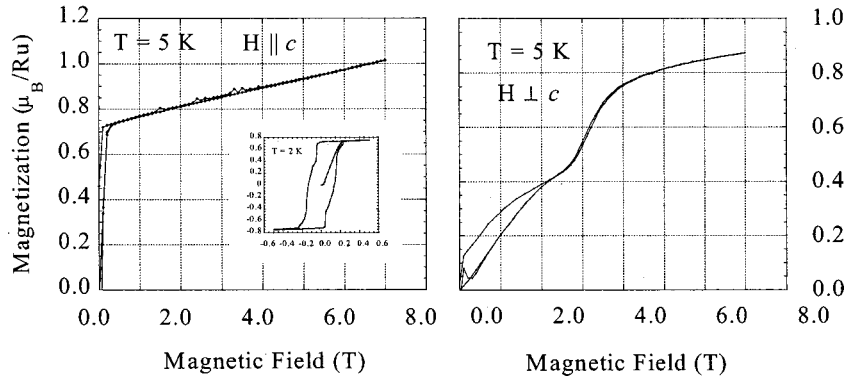


FIG. 3. Isothermal magnetization for a single crystal of $\text{Sr}_4\text{Ru}_3\text{O}_{10}$. The magnetic field was applied parallel (left) or perpendicular (right) to the crystallographic c axis, and the measurement temperature was 5 K. In the left frame (inset) is shown an expanded view of the low-field hysteresis with the magnetic field parallel to c (the easy axis) at 2 K.

$\text{Sr}_4\text{Ru}_3\text{O}_{10}$, and the measured magnetic properties thus reflected the presence of the triple-layer compound. This conclusion resolves the controversy concerning the magnetic properties of $\text{Sr}_3\text{Ru}_2\text{O}_7$ in favor of the properties reported for the floating-zone crystals: $\text{Sr}_3\text{Ru}_2\text{O}_7$ is an enhanced Pauli paramagnet.⁸ The conclusions of a previous report¹⁰ describing the magnetic properties of crystals identified to be $\text{Sr}_4\text{Ru}_3\text{O}_{10}$ by x-ray powder diffraction are also now called into question since those properties are very different from the properties we report here for structurally well-characterized single crystals of the same material.

Finally, we address the relationship between the magnetic and structural properties of $\text{Sr}_4\text{Ru}_3\text{O}_{10}$, and those of the other strontium ruthenates in the R - P series. Although single-layer Sr_2RuO_4 is structurally undistorted in the bulk, it has been shown¹⁵ by low-energy electron diffraction that it does have a surface structural distortion in which the RuO_6 octahedra rotate about the c axis by $9^\circ \pm 3^\circ$, and this distortion is predicted by first-principle calculations to lead to a ferromagnetic ground state in the near surface region. The authors of that study¹⁵ found that the observed rotation of 9° should lead to surface ferromagnetism with an ordered moment of $1.0 \mu_B/\text{Ru}$, rather similar to the bulk value we observe in $\text{Sr}_4\text{Ru}_3\text{O}_{10}$.

Other researchers¹⁶ have used density-functional calculations to examine the effect of rotations of the RuO_6 octahedra of double-layer $\text{Sr}_3\text{Ru}_2\text{O}_7$ on its magnetic properties, and predict a transition to ferromagnetic order in the orthorhombically distorted unit cell that results from these rotations.¹⁷ In $\text{Sr}_3\text{Ru}_2\text{O}_7$ the octahedra are rotated around the c axis by about 7° at room temperature,^{7,17} and although that material is not a ferromagnet, it is a strongly enhanced paramagnet.⁸ In fact, the application of hydrostatic pressure⁸ or a magnetic field¹⁴ induces ferromagnetism in $\text{Sr}_3\text{Ru}_2\text{O}_7$.

In $\text{Sr}_4\text{Ru}_3\text{O}_{10}$ the outer two layers of each triple layer have average rotations of 5.25° , less than those in $\text{Sr}_3\text{Ru}_2\text{O}_7$ and smaller than the “critical” value for ferromagnetism of 6.5 – 9° ,¹⁵ but the central layers have an average rotation of 10.6° , large enough to induce ferromagnetism. These are

room-temperature rotation angles,¹⁷ and using the observed behavior¹⁸ of $\text{Sr}_3\text{Ru}_2\text{O}_7$ as a guide they should increase at low temperatures. Furthermore, the RuO_6 octahedra in the outer layers are elongated¹⁹ to a degree (the ratio of the average out-of-plane to in-plane Ru-O distances is 1.0469) similar to the octahedra in *nearly ferromagnetic* $\text{Sr}_3\text{Ru}_2\text{O}_7$, whereas the octahedra in the central layer are nearly regular (1.0035), similar to the octahedra in *ferromagnetic* SrRuO_3 . The compound’s net magnetic properties might then be viewed as the result of magnetically coupling these different Ru sublattices. In the future, when large single crystals are available, it will be interesting to investigate the detailed behavior of the Ru^{4+} magnetic moments using neutron scattering.

In conclusion, we have determined the full structure and magnetic properties of $\text{Sr}_4\text{Ru}_3\text{O}_{10}$, the triple-layer member of the $\text{Sr}_{n+1}\text{Ru}_n\text{O}_{3n+1}$ Ruddlesden-Popper series. This material is a structurally distorted ferromagnet, and further study, including growth of high-purity single crystals by floating-zone techniques and characterization of their transport and neutron-scattering properties, will provide additional insight into the relationship between structure, (ferro)magnetism and superconductivity in the ruthenates.

Portions of this work were performed at the DuPont-Northwestern-Dow Collaborative Access Team (DND-CAT) Synchrotron Research Center of the Advanced Photon Source at Argonne National Laboratory. DND-CAT is supported by the E. I. DuPont de Nemours & Co., The Dow Chemical Company, the U.S. National Science Foundation through Grant No. DMR-9304725 and the State of Illinois through the Department of Commerce and the Board of Higher Education Grant No. IBHE HECA NWU 96. Use of the Advanced Photon Source was supported by the U.S. Department of Energy, Basic Energy Sciences, Office of Energy Research under Contract No. W-31-102-Eng-38. Work at the National High Magnetic Field Laboratory (NHMFL) was supported by the NHMFL In-House Research Program. We also thank Y. Maeno and S. Ikeda for useful discussions.

- ¹A. Callaghan, C. W. Moeller, and R. Ward, *Inorg. Chem.* **5**, 1572 (1966).
- ²I. I. Mazin and D. J. Singh, *Phys. Rev. B* **56**, 2556 (1997), and references therein.
- ³L. Antognazza, K. Char, T. H. Geballe, L. L. H. King, and A. W. Sleight, *Appl. Phys. Lett.* **63**, 7 (1993).
- ⁴Y. Maeno, H. Hashimoto, K. Yoshida, S. Nishizaki, T. Fujita, J. G. Bednorz, and F. Lichtenberg, *Nature (London)* **372**, 532 (1994).
- ⁵Y. Maeno, T. M. Rice, and M. Sigrist, *Phys. Today* **54** (1), 42 (2001).
- ⁶R. J. Cava, H. W. Zandbergen, J. J. Krajewski, W. F. Peck, Jr., B. Batlogg, S. Carter, R. M. Fleming, O. Zhou, and L. W. Rupp, Jr., *J. Solid State Chem.* **116**, 141 (1995).
- ⁷Q. Huang, J. W. Lynn, R. W. Erwin, J. Jarupatrakorn, and R. J. Cava, *Phys. Rev. B* **58**, 8515 (1998).
- ⁸S.-I. Ikeda, Y. Maeno, S. Nakatsuji, M. Kosaka, and Y. Uwatoko, *Phys. Rev. B* **62**, R6089 (2000).
- ⁹G. Cao, S. McCall, and J. E. Crow, *Phys. Rev. B* **55**, R672 (1997).
- ¹⁰G. Cao, S. K. McCall, J. E. Crow, and R. P. Guertin, *Phys. Rev. B* **56**, R5740 (1997).
- ¹¹It is important that neither $\text{Sr}_3\text{Ru}_2\text{O}_7$ nor Sr_2RuO_4 is ferromagnetic, so it is unlikely that the bulk magnetic data described in this paper are a result of the small degree of nonstoichiometry observed in these crystals. We also observed no evidence from NAA for Pt (from the crucible in which the crystals were grown) or Cl (from the SrCl_2 flux) in these crystals. It is interesting that a crystal of floating-zone $\text{Sr}_3\text{Ru}_2\text{O}_7$ (supplied by R. S. Perry and Y. Maeno) was also found to be Sr rich by NAA ($\text{Sr}/\text{Ru}=1.60 \pm 0.04$ vs 1.5 expected), but does not exhibit bulk ferromagnetism.
- ¹²We have also obtained neutron powder-diffraction patterns from ~ 0.5 g of crushed single crystals of nominally pure $\text{Sr}_3\text{Ru}_2\text{O}_7$.
- These patterns showed the crystals to actually be a mixture of 51 wt. % $\text{Sr}_4\text{Ru}_3\text{O}_{10}$, 34 wt. % $\text{Sr}_3\text{Ru}_2\text{O}_7$, and 15 wt. % Sr_2RuO_4 . At a temperature of 105 K additional intensities appeared at the positions of nuclear Bragg reflections which we indexed, based upon the single crystal x-ray unit cell, as due to the $\text{Sr}_4\text{Ru}_3\text{O}_{10}$ phase. The ordered moment determined from the neutron-diffraction data was $1.8(3) \mu_B/\text{Ru}^{4+}$ ion, aligned parallel to the c axis, in reasonable agreement with the magnitude and the direction of the ferromagnetic moment determined by SQUID magnetometry.
- ¹³G. Cao, S. McCall, M. Shepard, J. E. Crow, and R. P. Guertin, *Phys. Rev. B* **56**, 321 (1997).
- ¹⁴R. S. Perry, L. M. Galvin, S. A. Grigera, L. Capogna, A. J. Schofield, A. P. Mackenzie, M. Chiao, S. R. Julian, S.-I. Ikeda, S. Nakatsuji, Y. Maeno, and C. Pfleiderer, *Phys. Rev. Lett.* **86**, 2661 (2001); S. A. Grigera, R. S. Perry, A. J. Schofield, M. Chiao, S. R. Julian, G. G. Lonzarich, S. I. Ikeda, Y. Maeno, A. J. Millis, and A. P. Mackenzie, *Science* **294**, 329 (2001).
- ¹⁵R. Matzdorf, Z. Fang, Ismail, J. Zhang, T. Kimura, Y. Tokura, K. Terakura, and E. W. Plummer, *Science* **289**, 746 (2000).
- ¹⁶D. J. Singh and I. I. Mazin, *Phys. Rev. B* **63**, 165101 (2001).
- ¹⁷H. Shaked, J. D. Jorgensen, O. Chmaissem, S. Ikeda, and Y. Maeno, *J. Solid State Chem.* **154**, 361 (2000).
- ¹⁸H. Shaked, J. D. Jorgensen, S. Short, O. Chmaissem, S.-I. Ikeda, and Y. Maeno, *Phys. Rev. B* **62**, 8725 (2000).
- ¹⁹The energy differences between the $\text{Ru}^{4+} 4d^4 t_{2g}$ and e_g orbitals, and between the levels within the t_{2g} and e_g manifolds, is influenced by the individual Ru-O distances in each RuO_6 octahedron, whereas the conduction bandwidth and thus the density of states at the Fermi level (assuming $\text{Sr}_4\text{Ru}_3\text{O}_{10}$ is a metal) is sensitive to the RuO_6 rotations. This latter factor plays an important role in determining the stability of a ferromagnetic ground state through the Stoner-Wohlfarth criterion (see Refs. 8, 14, and 18 for detailed discussions of these points).